INTERNATIONAL JOURNAL FOR NUMERICAL METHODS IN FLUIDS, VOL. 23, 367–377 (1996)

HIGH-ORDER-ACCURATE DISCRETIZATION STENCIL FOR AN ELLIPTIC EQUATION

M. ARAD, A. YAKHOT* AND G. BEN-DOR

Pearlstone Center for Aeronautical Engineering Studies, Department of Mechanical Engineering, Ben-Gurion University of the Negev, Beersheva 84105, Israel

SUMMARY

The coefficients for a nine-point high-order-accurate discretization scheme for an elliptic equation $\nabla^2 u - \gamma^2 u = r_0$ (∇^2 is the two-dimensional Laplacian operator) are derived. Examples with Dirichlet and Neumann boundary condtions are considered. In order to demonstrate the high-order accuracy of the method, numerical results are compared with exact solutions.

KEY WORDS: discretization; high-order accuracy; duct flow

1. INTRODUCTION

The process of computational solution of a partial differential equation (PDE) involves a discretization procedure by which the continuous equation is replaced by a discrete algebraic equation. The discretization procedure consists of an approximation of the derivatives in the governing PDE by differences of the dependent variables which are computed only at discrete points (grid or mesh points). The discretization of the continuous problem inevitably introduces an error in computing the derivatives and, as a result, an error in the computational solution. In general, one starts with a given PDE and uses a discretization procedure for developing a finite difference equation (FDE). Then, with the aid of a Taylor series expansion about the node at which the derivative is evaluated, the PDE can be rewritten in the form PDE = FDE + TE, where the remainder TE is the truncation error. One can estimate the numerical solution error for a finite difference representation as the order of the leading term in the remainder, which can be considered as a close approximation to the error provided that the grid size is small. However, the complete evaluation of the numerical solution error must be based on comparison with the exact solution. The numerical solution error can be decreased if the leading derivative terms in the TE can be directly replaced using the differential equation. In this paper we develop a high-order-accurate nine-point discretization stencil for an elliptic equation which describes the problem of fully developed laminar flow in a rectangular duct and the torsional stress problem in elasticity.

2. DEFINITIONS

Computational domain G. Let a rectangle $G = \{0 \leqslant x \leqslant l_x, 0 \leqslant y \leqslant l_y\}$ be a two-dimensional computational domain. Let two discrete equally spaced sets ω_x and ω_y of points be defined by

$$\omega_x = \{x(i) = ih_x,\ i = 0, 1, \ldots, M,\ h_x M = l_x\}, \tag{1}$$

$$\omega_y = \{y(j) = jh_y,\ j = 0, 1, \ldots, N,\ h_y N = l_y\}. \tag{2}$$

*Corresponding author.

CCC 0271–2091/96/040367–11

Received May 1995
Revised December 1995

Computational grid Ω. Let a computational grid Ω on the domain G be a set of points defined by

$$\Omega = \omega_x \times \omega_y = \{\omega_{i,j} = (ih_x, jh_y), i = 0, 1, \ldots, M, j = 0, 1, \ldots, N\}.$$

Each (i, j)th node of the grid Ω refers to a point with co-ordinates $x(i)$ and $y(j)$ defined by equations (1) and (2). The grid Ω is equally spaced in the x- and y-direction.

Boundary and internal nodes. The nodes $[(0, j), \forall j]$, $[(M, j), \forall j]$, $[(i, 0), \forall i]$ and $[(i, N), \forall i]$ are boundary nodes. The nodes $[(i, j), i \neq 0 \text{ or } M, j \neq 0 \text{ or } N]$ are internal nodes.

Grid function $f_{i,j}$. Let a function $f(x,y)$ be defined on the domain G. A discrete function $f_{i,j} = f(x_i, y_i)$, where $x_i = x(i) \in \omega_x$ and $y_j = y(j) \in \omega_y$, is a grid representation of $f(x,y)$ on the computational grid Ω.

Nine-point stencil $\sigma_{ij}^{(9)}$. Let (i, j) be an internal node in the computational grid Ω. Let a nine-point discretization stencil $\sigma_{ij}^{(9)}$ about a central node (i, j) be defined by

$$\sigma_{ij}^{(9)} = \{\omega_{p,q}, p = i-1, i, i+1, q = j-1, j, j+1\}, \tag{3}$$

where $\omega_{p,q} \in \Omega$.

Taylor series expansion on $\sigma_{ij}^{(9)}$. Let a discrete function $f_{i,j}$ be defined on $\sigma_{ij}^{(9)}$. A Taylor series expansion of $f_{i,j}$ about the central (i, j) node is

$$f_{i+p,j+q} = f_{i,j} + \sum_{m=1}^{\infty} \mathscr{D}_{p,q}^{m} f_{i,j}, \tag{4}$$

$$\mathscr{D}_{p,q}^{m} = \frac{1}{m!}(ph_x D_x + qh_y D_y)^m, \quad p, q = -1, 0, 1.$$

In equation (4), $D_x^m = \partial/\partial x^m$ and $D_y^m = \partial/\partial y^m$ are differential operators.

Discrete equation on $\sigma_{ij}^{(9)}$. Let any linear relation between nine discrete values $u_{p,q}$ computed on $\sigma_{ij}^{(9)}$, i.e.

$$\sum_{p=i-1}^{i+1} \sum_{q=j-1}^{j+1} \hat{a}_{pq} u_{p,q} = 0, \tag{5}$$

be a discrete equation for a function $u(x,y)$. Hereafter, coefficients $\hat{a}_{pq}$ will be called the $\sigma_{ij}^{(9)}$-stencil coefficients.

Modified equation on $\sigma_{ij}^{(9)}$. We consider a linear partial differential equation of the second order in two independent variables:

$$L^{(2)}u + L^{(1)}u + L^{(0)}u + f(x,y) = 0. \tag{6}$$

In equation (6) the operators $L^{(0)}$, $L^{(1)}$ and $L^{(2)}$ are

$$L^{(0)} = c, \qquad L^{(1)} = c_1 D_x + c_2 D_y, \qquad L^{(2)} = a_{11} D_x^2 + 2a_{12} D_x D_y + a_{22} D_y^2, \tag{7}$$

where c, c_1, c_2 and a_{11}, a_{12}, a_{22} are known coefficients and $f(x,y)$ is a known function. Let us substitute Taylor series expansions (4) about the node $(i, j) \in \sigma_{ij}^{(9)}$ into a discrete equation (5) for each $u_{p,q}$. The Taylor series expansions (4) include the differential operators and we can formally rearrange the discrete equation into the form

$$\hat{L}^{(2)} u_{i,j} + \hat{L}^{(1)} u_{i,j} + \hat{L}^{(0)} u_{i,j} + f_{i,j} = TE. \tag{8}$$

Here $\hat{L}^{(0)}$, $\hat{L}^{(1)}$ and $\hat{L}^{(2)}$ are operators given by

$$\hat{L}^{(0)} = \hat{c}, \qquad \hat{L}^{(1)} = \hat{c}_1 D_x + \hat{c}_2 D_y, \qquad \hat{L}^{(2)} = \hat{a}_{11} D_x^2 + 2\hat{a}_{12} D_x D_y + \hat{a}_{22} D_y^2, \tag{9}$$

where the coefficients $\hat{c}, \hat{c}_1, \hat{c}_2$ and $\hat{a}_{11}, \hat{a}_{12}, \hat{a}_{22}$ depend on the coefficients $\hat{a}_{pq}$ of the $\sigma_{ij}^{(9)}$-stencil. The right-hand side of equation (8), which is called the *truncation error TE*, consists of high-order terms (derivatives) and can be expressed as

$$TE = \sum_{r=s\geqslant 3}^{\infty} \hat{L}^{(r)} u_{i,j}, \qquad \hat{L}^{(r)} = \sum_{m=0}^{r} \alpha_m h_x^m h_y^{r-m} D_x^m D_y^{r-m}. \tag{10}$$

If the $\sigma_{ij}^{(9)}$-stencil coefficients $\hat{a}_{pq}$ are chosen such that $\hat{L}^{(2)} = L^{(2)}, \hat{L}^{(1)} = L^{(1)}$ and $\hat{L}^{(0)} = L^{(0)}$, then equation (8) is called the *modified equation*[1] of equation (6). It is the PDE that is actually solved when the original equation (6) is discretized using a finite difference approach. The right-hand side (*TE*) is the difference between the original PDE and its finite difference approximation (FDE). The lowest-order term of *TE* gives the accuracy order of the discretization method applied to the original PDE. For example, the truncation error in equation (10) is $O(h^s)$.

We recall two ways of increasing the accuracy order of a finite difference equation on a given discretization stencil. (a) The stencil coefficients $\hat{a}_{pq}$ are chosen to make the accuracy order (s in equation (10)) as high as possible (in other words, as many as possible first terms of *TE* are set to zero). (b) Using the original PDE, as many as possible first terms of *TE* are expressed in terms of the original PDE operators ($L^{(0)}, L^{(1)}$ and $L^{(2)}$ in equation (6)) and are moved to the left-hand side of the discrete equation; then the discretization stencil coefficients $\hat{a}_{pq}$ are chosen in order that the discrete equation will be the modified version of the original PDE.

3. NINE-POINT STENCIL FOR $(\nabla^2 - \gamma^2)u = r_0$

We consider an elliptic equation

$$\nabla^2 u - \gamma^2 u = (D_x^2 + D_y^2)u - \gamma^2 u = r_0, \tag{11}$$

where γ and r_0 are constants and $\nabla^2 = D_x^2 + D_y^2$ is the two-dimensional Laplacian operator ($D_x^2 = \partial/\partial x^2, D_y^2 = \partial/\partial y^2$). Our goal is to convert equation (11) to a high-order-accurate difference equation written at each internal node $(i, j,) \in \sigma_{ij}^{(9)}$.

We choose the discrete equation for (11) on the nine-point $\sigma_{ij}^{(9)}$-stencil in the form

$$au_{i,j} + bS_{i,j}^{(xy)} + cS_{i,j}^{(x)} + dS_{i,j}^{(y)} = r_0, \tag{12}$$

where

$$S_{i,j}^{(xy)} = u_{i-1,j-1} + u_{i-1,j+1} + u_{i+1,j-1} + u_{i+1,j+1},$$
$$S_{i,j}^{(x)} = u_{i-1,j} + u_{i+1,j}, \qquad S_{i,j}^{(y)} = u_{i,j-1} + u_{i,j+1}.$$

Owing to the symmetry of the sums $S_{i,j}^{(xy)}, S_{i,j}^{(x)}$ and $S_{i,j}^{(y)}$ about the central node (i, j), upon substituting the Taylor series expansions into equation (12), the resulting equation consists of only even-order derivatives: $D_x^2, D_y^2, D_x^4, D_x^2D_y^2, D_y^4, D_x^6, D_x^2D_y^4, \ldots$. The derivation of the $\sigma_{ij}^{(9)}$-stencil coefficients is described in Appendix I. The coefficients are summarized in Table I. The derivation is performed using a symbolic operator procedure. The same expressions for the coefficients could be obtained using the differential finite difference method presented by Arad *et al.*[2] The truncation error for $h_x \neq h_y$ is $O(h_x^4, h_x^2h_y^2, h_y^4)$, while for $h_x = h_y = h$ it is $O(h^6)$. Coefficients for the last two cases ($\gamma = 0$) are known as 'a nine-point formula' for the Laplace operator.[1] This formula provides high-order accuracy for the Laplace equation. However, the truncation error is only $O(h_x^2, h_y^2)$ or $O(h^4)$ if the same coefficients are used for discretization of the first two cases with $\gamma \neq 0$. The coefficients of the discretization scheme, which have been derived using the original PDE and are presented in Table I, enable us to increase the accuracy up to the fourth or sixth order.

Table I. Summary of nine-point discretization stencil coefficients, $A_s = s^2/2! + (s^4/4!)\gamma^2 + (s^6/6!)\gamma^4$

Case	a	b	c	d
$\gamma \neq 0, h_x \neq h_y$	$-\gamma^2 - \dfrac{1}{A_{h_x}} - \dfrac{1}{A_{h_y}} + 4b$	$\dfrac{A_{h_y} h_x^4(20 + h_x^2\gamma^2) + A_{h_x} h_y^4(20 + h_y^2\gamma^2)}{20A_{h_x}A_{h_y}h_x^2h_y^2[24 + (h_x^2 + h_y^2)\gamma^2]}$	$\dfrac{1}{2A_{h_x}} - 2b$	$\dfrac{1}{2A_{h_y}} - 2b$
$\gamma \neq 0, h_x = h_y = h$	$-\gamma^2 - \dfrac{2}{A_h} + 4b$	$\dfrac{20 + h^2\gamma^2}{20A_h(12 + h^2\gamma^2)}$	$\dfrac{1}{2A_h} - 2b$	$\dfrac{1}{2A_h} - 2b$
$\gamma = 0, h_x \neq h_y$	$-\dfrac{5(h_x^2 + h_y^2)}{3h_x^2h_y^2}$	$\dfrac{h_x^2 + h_y^2}{12h_x^2h_y^2}$	$\dfrac{5h_y^2 - h_x^2}{6h_x^2h_y^2}$	$\dfrac{5h_x^2 - h_y^2}{6h_x^2h_y^2}$
$\gamma = 0, h_x = h_y = h$	$-\dfrac{10}{3h^2}$	$\dfrac{1}{6h^2}$	$\dfrac{2}{3h^2}$	$\dfrac{2}{3h^2}$

The nine-point stencil developed in this section is appropriate for internal nodes of the computational domain. For Dirichlet boundary conditions the only source of errors in the numerical solution arises from the discretization of the governing equation. Neumann boundary conditions require discretization of the derivatives at the boundary. In general it is necessary to express Neumann condition in a discrete form with at least the same truncation error as the discretization scheme used for the governing equation. The lower accuracy of the solution at the boundary will contaminate the accuracy of the numerical solution in the interior nodes. In Appendix II we present the high-order-accurate discretization of the Neumann boundary condition for equation (11) using the fictitious (dummy) nodes approach.

4. NUMERICAL RESULTS

In this section we present numerical results which were obtained using the high-order discretization stencil and compare the accuracy with exact solutions.

For $\gamma = 0$ the problem defined by equation (11) is equivalent to the problem of fully developed laminar duct flow[3] and to the torsional stress problem in elasticity.[4] Fletcher[5] considered this problem and presented a special program (DUCT) for its numerical solution. Different (finite element and finite difference) methods for discretization are implemented by the programme DUCT. For the cases with $\gamma \neq 0$ which are considered in this section, we slightly modified the programme DUCT. The high-order-accurate discretization procedure developed here does not change the general structure of the matrix involved in the programme DUCT. Only the matrix coefficients should be calculated according to the nine-point $\sigma_{ij}^{(9)}$-stencil. Therefore the convergence rate of any solution method (direct or iterative) applied to the problem and discussed in detail by Fletcher[5] is not affected by the suggested discretization procedure. However, owing to the high-order-accurate discretization, the suggested scheme provides a significant improvement. The computational work required to achieve a given accuracy with the nine-point $\sigma_{ij}^{(9)}$-stencil is orders of magnitude less than the computational efforts with the standard five-point finite difference discretization, because a much coarser grid is needed for the computation.

In all our calculations the Gauss–Seidel iterative method with successive overrelaxation implemented in the programme DUCT[5] has been used. We use the relaxation parameter $\omega = 1{\cdot}65$. The accuracy of the results (numerical versus exact) is analysed with grid refinement.

Case 1: $\gamma^2 = \mathbf{H}^2$, $\mathbf{r}_0 = -\mathbf{1}$, *duct flow*

We consider the two-dimensional problem

$$\frac{\partial^2 u}{\partial x^2} + \frac{\partial^2 u}{\partial y^2} - H^2 u = -1, \qquad |x| \leqslant a, \qquad |y| \leqslant b, \qquad u(\pm a, y) = u(x, \pm b) = 0. \tag{13}$$

For $H \neq 0$ the problem defined by equation (13) is equivalent to the problem of steady, fully developed magnetohydrodynamic laminar flow in a rectangular duct with non-conducting walls, where H is the Hartmann number. The exact solution for this problem was first obtained by Shercliff.[6] The exact solution of equation (13) is readily obtained using the method of separation of variables and there are different forms of this solution. Here we present the solution in the form

$$u(x, y) = \sum_{m=1}^{\infty} U_m(x) \sin[\lambda_m(y + b)],$$

$$U_m(x) = \frac{4}{\pi(2m-1)\mu_m^2}\left(1 - \frac{\cosh(\mu_m x)}{\cosh(\mu_m a)}\right), \qquad \mu_m^2 = H^2 + \lambda_m^2, \qquad \lambda_m = \frac{\pi(2m-1)}{2b}. \tag{14}$$

The main feature of the exact solution given by equation (14) is a very severe near-wall gradient at high Hartmann numbers H. From the computational point of view, for such boundary layer solutions a certain grid refinement should be used as the near-boundary gradient becomes sharper (increasing H). The order of the solution error coincides with the order of the truncation error if the grid spacing is sufficiently small. In the case at hand, at high values of H one can expect that the estimated numerical solution error will be achieved only for a very fine grid.

In Figure 1, for different grid spacings, we plot the numerical solution error $Error = \|u_{ij} - u_{i\,j}^{(e)}\|_{\text{rms}}$, where the exact solution $u_{i\,j}^{(e)}$ is evaluated from equation (14) at each (i, j)th node. We consider a square ($a = b = 1$) duct and hence $h_x = h_y = h = 2/N$. Figure 1 clearly illustrates the superiority of the suggested high-order discretization. Let us assume that an engineering accuracy of 0·1% (i.e. $Error = 10^{-3}$ in Figure 1) in the RMS error of the computational solution is required. Then, as can be deduced from Figure 1, for the severe case of $H = 10$, i.e. a sharp near-wall gradient, $h \approx 1/3$ is required if the presently proposed $\sigma_{i\,j}^{(9)}$-stencil is used, in contrast with $h \approx 1/35$ which is required if the standard five-point discretization is applied. Since, as mentioned above, $h = 2/N$, this implies that the proposed discretization scheme enables a reduction of the mesh from 70×70 to 6×6 while keeping the error at the 0·1% level.

It should be noted that it is difficult to conduct an accurate comparison between the numerical and exact solutions of the problem given by equation (13), because the rate of convergence of the infinite series (14) *decreases* for higher values of H. One can see that the standard five-point finite difference discretization scheme provides a numerical solution error of $O(h^2)$ as predicted (the slope of the five-point FD curves is equal to 2). The high-order $\sigma_{i\,j}^{(9)}$-stencil discretization gives an accuracy of approximately $O(h^3)$ and not of $O(h^6)$ as predicted. This discrepancy deserves an explanation. The $O(h^6)$ accuracy will apparently be achieved at $h < 0{\cdot}01$ (i.e. $-\log(h) > 2$ in Figure 1). However, the slow convergence of the infinite series given by equation (14) requires accounting for many terms in the series (especially for high values of H). This in turn leads to an inevitable accumulation of machine round-off errors. In addition, the very small expected accuracy (less than $O(10^{-12})$) makes the numerical implementation very difficult.

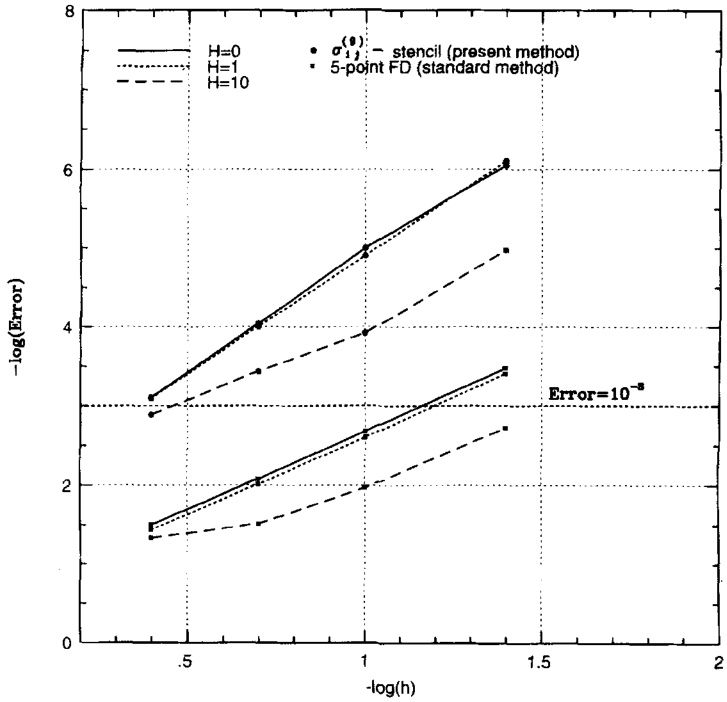

Figure 1. Numerical solution error for different computational meshes (Case 1, duct flow)

Case 2: $\gamma^2 = \mathbf{H}^2$, $\mathbf{r}_0 = -\mathbf{1}$, *Dirichlet boundary condition, soluble example*

In order to demonstrate the high-order solution accuracy of the proposed $\sigma_{ij}^{(9)}$-stencil, we consider the two-dimensional problem

$$\frac{\partial^2 u}{\partial x^2} + \frac{\partial^2 u}{\partial y^2} - H^2 u = -1, \quad 0 \leqslant x \leqslant 1, \quad 0 \leqslant y \leqslant 1,$$

$$u(0, y) = u(1, y) = \frac{1}{H^2}, \qquad u(x, 0) = \frac{1}{H^2}, \qquad u(x, 1) = \sin(\pi x) + \frac{1}{H^2}. \tag{15}$$

The exact solution is given by

$$u(x, y) = \frac{\sin(\pi x)\sinh(\alpha y)}{\sinh(\alpha)} + \frac{1}{H^2}, \qquad \alpha^2 = \pi^2 + H^2. \tag{16}$$

In Figure 2, as in the previous example, we plot the numerical solution error $Error = \|u_{ij} - u_{ij}^{(e)}\|_{\mathrm{rms}}$, where $u^{(e)}$ is the exact solution evaluated from equation (16) at each (i, j)th node. The results obtained with the suggested $\sigma_{ij}^{(9)}$-stencil clearly show the sixth-order solution accuracy, $Error = O(h^6)$, on a square mesh, $h_x = h_y = h$. On an unequally spaced mesh ($h_x = 2h_y$) the numerical solution error with the suggested $\sigma_{ij}^{(9)}$-stencil discretization increases and becomes of the fourth order. The five-point FD discretization gives a second-order solution accuracy.

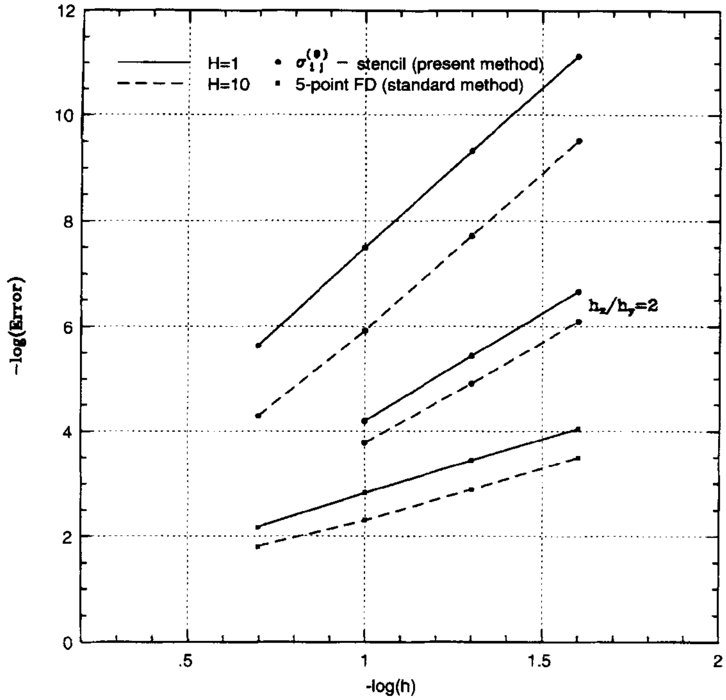

Figure 2. Numerical solution error for different computational meshes (Case 2, Dirichlet condition, soluble example)

Case 3: $\gamma^2 = \mathbf{H}^2, \mathbf{r}_0 = -1$, *Neumann boundary condition, soluble example*

In order to demonstrate the effect of the accuracy of the Neumann boundary condition discrete approximation on the numerical solution error, we consider the two-dimensional problem

$$\frac{\partial^2 u}{\partial x^2} + \frac{\partial^2 u}{\partial y^2} - H^2 u = -1, \quad 0 \leqslant x \leqslant 1, \quad 0 \leqslant y \leqslant 1,$$

$$u(0,y) = u(1,y) = \frac{1}{H^2}, \qquad u(x,0) = \frac{1}{H^2}, \qquad u_y(x,1) = \alpha \sin(\pi x)\coth(\alpha). \tag{17}$$

The exact solution of the problem is given by

$$u(x,y) = \frac{\sin(\pi x)\sinh(\alpha y)}{\sinh(\alpha)} + \frac{1}{H^2}, \qquad \alpha^2 = \pi^2 + H^2. \tag{18}$$

For the numerical solution we use a square mesh, $h_x = h_y = h$. In Figure 3 we plot the numerical solution error $Error = \|u_{ij} - u_{ij}^{(e)}\|_{\mathrm{rms}}$. Only the calculations obtained with the suggested nine-point $\sigma_{ij}^{(9)}$-stencil and the sixth-order-accurate Neumann condition discretization result in a sixth-order solution accuracy, $Error = O(h^6)$. With the second-order-accurate discretization of the Neumann condition the numerical solution error with the suggested nine-point $\sigma_{ij}^{(9)}$-stencil discretization increases and becomes of the second-order only. In this case the low accuracy of the boundary derivative discrete approximation overrides the high-order accuracy provided by the scheme with the nine-point $\sigma_{ij}^{(9)}$-stencil. The five-point finite difference discretization gives a second-order solution accuracy as expected.

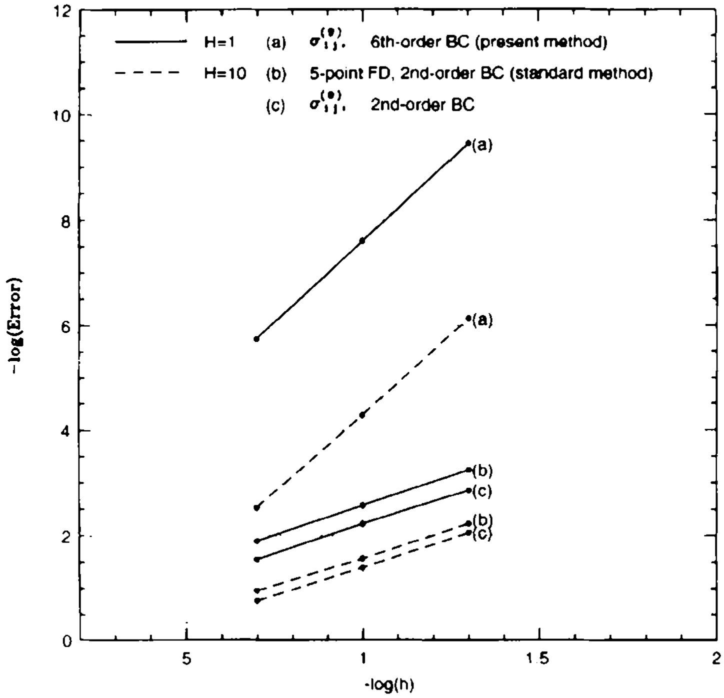

Figure 3. Numerical solution error for different computational meshes (Case 3, Neumann condition, soluble example)

5. CONCLUSIONS

We derive the coefficients for a nine-point discretization scheme for an elliptic equation $\nabla^2 u - \gamma^2 u = r_0$($\nabla^2$ is the two-dimensional Laplacian operator). The truncation error for the suggested scheme is of the sixth order, $O(h^6)$, on a square mesh ($h_x = h_y = h$) and of the fourth order, $O(h_x^4, h_x^2 h_y^2, h_y^4)$, on an unequally spaced mesh. The performance of the suggested discretization scheme is demonstrated on three examples and is compared with that of the standard five-point discretization formula. Examples with Dirichlet and Neumann boundary conditions are considered to demonstrate the high-order accuracy of the method.

APPENDIX I: DERIVATION OF THE $\sigma^{(9)}_{ij}$-STENCIL COEFFICIENTS

Let

$$au_{i,j} + bS^{xy}_{i,j} + cS^{(x)}_{i,j} + dS^{(y)}_{i,j} = r_0 \tag{19}$$

be a discrete equation on the nine-point $\sigma^{(9)}_{ij}$-stencil, where

$$S^{(xy)}_{i,j} = u_{i-1,j-1} + u_{i-1,j+1} + u_{i+1,j-1} + u_{i+1,j+1},$$

$$S^{(x)}_{i,j} = u_{i-1,j} + u_{i+1,j}, \qquad S^{(y)}_{i,j} = u_{i,j-1} + u_{i,j+1}. \tag{20}$$

The Taylor series expansions on $\sigma_{ij}^{(9)}$ are

$$u_{i\pm 1,j\pm 1} = u_{i,j} + \sum_{m=1}^{\infty} \frac{1}{m!}(\pm h_x D_x \pm h_y D_y)^m u_{i,j}. \tag{21}$$

Substituting expansions (21) into (20) leads to

$$S_{i,j}^{(xy)} = 4u_{i,j} + 4\sum_{m=1}^{\infty}\sum_{n=0}^{m} \frac{h_x^{2m-2n}h_y^{2n}}{(2m-2n)!(2n)!} D_x^{2m-2n} D_y^{2n} u_{i,j},$$

$$S_{i,j}^{(x)} = 2u_{i,j} + 2\sum_{m=1}^{\infty} \frac{h_x^{2m}}{(2m)!} D_x^{2m} u_{i,j}, \qquad S_{i,j}^{(y)} = 2u_{i,j} + 2\sum_{m=1}^{\infty} \frac{h_y^{2m}}{(2m)!} D_y^{2m} u_{i,j}. \tag{22}$$

Substituting (22) into (19) and keeping derivatives up to the sixth order in the left-hand side give

$$\Bigg[(4b+2c)\left(\frac{h_x^2}{2!}D_x^2 + \frac{h_x^4}{4!}D_x^4 + \frac{h_x^6}{6!}D_x^6\right) + (4b+2d)\left(\frac{h_y^2}{2!}D_y^2 + \frac{h_y^4}{4!}D_y^4 + \frac{h_y^6}{6!}D_y^6\right)$$

$$+4b\left(\frac{h_x^2h_y^2}{2!2!}D_x^2D_y^2 + \frac{h_x^4h_y^2}{4!2!}D_x^4D_y^2 + \frac{h_x^2h_y^4}{2!4!}D_x^2D_y^4\right) + (a+4b+2c+2d)\Bigg]u_{i,j} = r_0 + TE. \tag{23}$$

Using (11) enables one to rewrite the high-order derivative operators in the left-hand side of (23) as

$$D_x^4 = \gamma^2 D_x^2 - D_x^2 D_y^2, \qquad D_y^4 = \gamma^2 D_y^2 - D_x^2 D_y^2,$$

$$D_x^6 = \gamma^4 D_x^2 - \gamma^2 D_x^2 D_y^2 - D_x^4 D_y^2, \qquad D_y^6 = \gamma^4 D_y^2 - \gamma^2 D_x^2 D_y^2 - D_x^2 D_y^4. \tag{24}$$

Substituting (24) into (23) gives

$$(\hat{a}_{11}D_x^2 + 2\hat{b}D_x^2D_y^2 + \hat{a}_{22}D_y^2 + \hat{a}_{00})u_{i,j} + (g_{42}D_x^4D_y^2 + g_{24}D_x^2D_y^4)u_{i,j} = r_0 + TE, \tag{25}$$

where $g_{42} = g(h_x, h_y; b, c, d)$ and $g_{24} = g(h_y, h_x; b, c, d)$. We note that for an equally spaced grid, $h_x = h_y$, owing to $x \leftrightarrow y$ symmetry of the elliptic equation, $c = d$ in (19) and hence $g_{42} = g_{24}$. Therefore it is useful to rewrite the second term on the left-hand side of (25) as

$$g_{42}D_x^4D_y^2 + g_{24}D_x^2D_y^4 \equiv \frac{g_{42}+g_{24}}{2}(D_x^4D_y^2 + D_x^2D_y^4) + \frac{g_{42}-g_{24}}{2}(D_x^4D_y^2 - D_x^2D_y^4)$$

$$= \gamma^2\frac{g_{42}+g_{24}}{2}D_x^2D_y^2 + \frac{g_{42}-g_{24}}{2}(D_x^4D_y^2 - D_x^2D_y^4), \tag{26}$$

because the second term in (26) vanishes on the equally spaced grid. Adding the first term of (26) to the mixed derivative term of (25) and moving the second one (which is actually the leading term of the truncation error) to the right-hand side of (25) complete the rearrangement of the discrete equation, which now reads

$$(\hat{a}_{11}D_x^2 + 2\hat{a}_{12}D_x^2D_y^2 + \hat{a}_{22}D_y^2 + \hat{a}_{00})u_{i,j} = r_0 + TE, \tag{27}$$

where the truncation error is estimated as

$$TE \approx \frac{g_{42}-g_{24}}{2}(D_x^4D_y^2 - D_x^2D_y^4)u_{i,j}. \tag{28}$$

The coefficients $\hat{a}_{pq}$ in (27) depend on the grid spacing h_x, h_y and on the $\sigma_{ij}^{(9)}$-stencil coefficients a, b, c, d. In order for (27) to become the modified equation of the original equation (11), we require

$$\hat{a}_{00} = -\gamma^2, \qquad \hat{a}_{11} = 1, \qquad \hat{a}_{12} = 0, \qquad \hat{a}_{22} = 1, \tag{29}$$

which is a linear system for four unknown coefficients a, b, c, d. We omit simple algebra and summarize the coefficients in Table I.

APPENDIX II: NEUMANN BOUNDARY CONDITIONS

Assume that the Neumann boundary condition $du/dy|_{y=0} = g(x)$ is imposed at the boundary $y = 0$. Let

$$au_{i,0} + bS_{i,0}^{(xy)} + cS_{i,0}^{(x)} + dS_{i,0}^{(y)} = r_0 \tag{30}$$

be the nine-point $\sigma_{ij}^{(9)}$-stencil applied at a boundary point $(i, 0)$, where

$$S_{i,0}^{(x,y)} = u_{i-1,-1} + u_{i-1,1} + u_{i+1,-1} + u_{i+1,1},$$
$$S_{i,0}^{(x)} = u_{i-1,0} + u_{i+1,0}, \qquad S_{i,0}^{(y)} = u_{i,-1} + u_{i,1}.$$

Here $(k, -1)$, $k = i-1, i, i+1$, denote the fictitious (dummy) nodes which are used in the nine-point $\sigma_{ij}^{(9)}$-stencil and lie outside the computational domain. The Taylor series expansions for the dummy nodes read

$$u_{k,\pm1} = u_{k,0} + \sum_{m=1}^{\infty} \frac{(\pm1)^m}{m!} h^m D_{y0}^m u_{k,0}, \qquad D_{y0}^m u_{k,0} \equiv D_{y0}^m u = , \frac{d^m u}{dx^m}\bigg|_{y=0}, \tag{31}$$

where, and hereafter, $h_y = h$, $k = i-1, i, i+1$. From (31) we have

$$u_{k,1} - u_{k,-1} = 2 \sum_{m=1}^{\infty} \frac{h^{2m-1}}{(2m-1)!} D_{y0}^{2m-1} u_{k,0}. \tag{32}$$

Using (11) enables one to rewrite the odd-order y-derivative operators in the recurrent form

$$D_y^{2m-1} u = (\gamma^2 - D_x^2) D_y^{2m-3} u, \quad m = 2, 3, \ldots. \tag{33}$$

Applying (33) at the boundary point $y = 0$ gives

$$D_{y0}^{2m-1} u = (\gamma^2 - D_x^2)^{m-1} g(x), \quad m = 2, 3, \ldots. \tag{34}$$

From (32) and (34) we obtain explicit expressions for the dummy nodes:

$$u_{k-1} = u_{k,1} - 2 \sum_{m=1}^{\infty} \frac{h^{2m-1}}{(2m-1)!} (\gamma^2 - D_x^2)^{m-1} g(x), \quad k = i-1, i, i+1. \tag{35}$$

For the sixth-order-accurate case we have

$$u_{k,-1} = u_{k,1} - 2 \sum_{m=1}^{3} \frac{h^{2m-1}}{(2m-1)!} (\gamma^2 - D_x^2)^{m-1} g(x) + O(h^6), \quad k = i-1, i, i+1. \tag{36}$$

Substituting expressions (36) for the dummy nodes into (30) gives the sixth-order-accurate discretization of the Neumann boundary condition for (11).

REFERENCES

1. D. A. Anderson, J. C. Tannehill and R. H. Pletcher, *Computational Fluid Mechanics and Heat Transfer*, Hemisphere, Washington, D.C., 1984.
2. M. Arad, R. Segev and G. Ben-Dor, 'Improved finite difference method for equilibrium problems based on differentiation of the partial differential equations and the boundary conditions', *Int. j. numer methods eng.*, **38**, 1831–1853 (1995).
3. F. M. White, *Viscous Fluid Flow*, McGraw-Hill, New York, 1974.
4. I. S. Sokolnikoff, *Mathematical Theory of Elasticity*, McGraw-Hill, New York, 1946.
5. C. A. J. Fletcher, *Computational Techniques for Fluid Dynamics*, Vol. 1, Springer, New York, 1988.
6. J. A. Shercliff, 'Steady motion of conducting fluids in pipes under transverse magnetic fields', *Proc. Camb. Philos. Soc.*, **49**, 136–144 (1953).